

# Novel Zinc Oxide Nanostructures Discovery by Electron Microscopy

Zhong Lin Wang\*

School of Materials Science and Engineering, Georgia Institute of Technology,  
Atlanta, GA 30332-0245, USA

**Abstract.** Zinc oxide is an important semiconducting and piezoelectric material. Structurally, due to the three types of fast growth direction:  $\langle 0001 \rangle$ ,  $\langle 01\bar{1}0 \rangle$  and  $\langle 2\bar{1}\bar{1}0 \rangle$  as well as the  $\pm(0001)$  polar surfaces, a diversity group of ZnO nanostructures have been grown in our laboratory: including nanocombs, nanosaws, nanosprings, nanorings, nanobows and nanopropellers. This article reviews our recent progress in the synthesis and characterization of the polar surface induced ZnO nanostructures and their growth mechanisms.

## 1. Introduction

As inspired by the discovery of oxide nanobelts [1,2], research in functional oxide based one-dimensional nanostructures is rapidly expanding and becoming a forefront research in nanotechnology. Field effect transistors [3] and ultra-sensitive nano-size gas sensors [4], nanoresonators [5] and nanocantilevers [6] have been fabricated based on individual nanobelts. Thermal transport along a nanobelt has been measured [7]. Zinc oxide (ZnO), is the most typical and successful example of an oxide nanobelt. Zinc oxide has three key advantages. First, it is a semiconductor, with a direct wide band gap of 3.37 eV and a large excitation binding energy (60 meV). It is an important functional oxide, exhibiting near-UV emission and visible light transparency. Second, due to non-central symmetry, it is a piezoelectric, which is a key phenomenon in building electro-mechanical coupled sensors and transducers. Finally, ZnO is bio-safe and biocompatible, and it can be directly used for biomedical applications without coating. With these unique characteristics, ZnO is one of the most important nanomaterials for future research and applications.

## 2. Novel nanostructures of ZnO

Zinc oxide has a hexagonal structure (space group  $C6mc$ ) with lattice parameters of  $a = 0.3296$  and  $c = 0.52065$  nm. The structure of ZnO can be simply described as a number of alternating planes composed of tetrahedrally coordinated  $O^{2-}$  and  $Zn^{2+}$  ions, stacked along the  $c$ -axis. The most important polar surface for ZnO is the basal plane. The oppositely charged ions produce positively charged Zn-(0001) and negatively charged O-(000 $\bar{1}$ ) polar surfaces. As a result of surface atomic termination and surface polar charges, a wide range of nanostructures has been produced.

---

\* zhong.wang@mse.gatech.edu

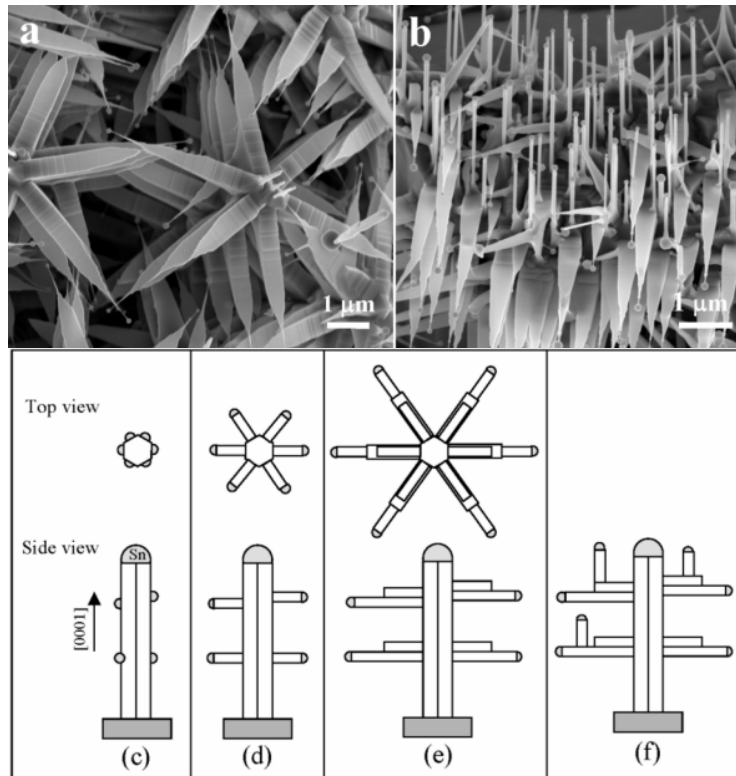


Figure 1. (a, b) SEM images of aligned nanopropellers. (c-f) Mechanistic steps of the vapor-liquid-solid growth process of the ZnO nanopropellers.

### 2.1. Aligned nanopropellers

We used a mixture of ZnO and SnO<sub>2</sub> powders in a weight ratio of 1:1 as the source material to grow complex ZnO nanostructures [8,9]. Figure 1a shows an SEM image of the as-synthesized products with a feature consisting of sets of axial nanowires, surrounded by radial oriented “tadpole-like” nanostructures. The ribbon shaped branches have spherical balls at the tips (Figure 1a). The ribbon branches have a fairly uniform thickness and their surfaces are rough with steps. Secondary growth on these propeller surface leads to aligned nanowires (Fig. 1b).

It is known that SnO<sub>2</sub> can decompose into Sn and O<sub>2</sub> at high temperature, thus, the growth of the nanowire-nanoribbon junction arrays is the result of the vapor-liquid-solid (VLS) growth process in which the Sn catalyst particles are responsible for initiating and leading the growth of ZnO nanowires and nanobelts. The growth of the novel nanopropeller structure presented here can be separated into two stages. The first stage is a fast growth of the ZnO axial nanowire along [0001] (Fig. 1c). The growth rate is so high that a slow increase in the size of the Sn droplet has little influence on the diameter of the nanowire, thus the axial nanowire has a fairly uniform shape along the growth direction. The second stage of the growth is the nucleation and epitaxial growth of the nanoribbons due to the arrival of tiny Sn droplets onto the ZnO nanowire surface (Fig. 1d). This stage is much slower than the first stage and the lengths of the nanoribbons are uniform and much shorter than that of the nanowire because of the different growth axis. Since Sn is in liquid state at the growth temperature, it tends to adsorb the newly arriving Sn species and grows into a larger sized particle (i.e. coalescing). Therefore, the width of the nanoribbon increases as the size of the Sn particle at the tip becomes larger, resulting in the formation of the tadpole-like structures observed in TEM (Fig. 1e). The Sn liquid droplets deposited onto the ZnO nanowire lead to the simultaneous growth of the ZnO nanoribbons along the six equivalent growth directions:  $\pm[10\bar{1}0]$ ,

$\pm[0\bar{1}10]$  and  $\pm[\bar{1}100]$ . Secondary growth along  $[0001]$  results in the growth of aligned nanowires on the surfaces of the propellers (Fig. 1f).

## 2.2. Spiral nanostructures and nanosprings

Due to differences in the surface energies of  $\{0001\}$ ,  $\{01\bar{1}0\}$  and  $\{2\bar{1}\bar{1}0\}$  planes, freestanding nanobelts and nanowires of ZnO are usually dominated by the lower energy, non-polar surfaces such as  $\{01\bar{1}0\}$  and  $\{2\bar{1}\bar{1}0\}$ . Recently, ZnO nanobelts dominated by the  $\{0001\}$  polar surfaces have been grown [10]. The nanobelt grows along  $[2\bar{1}\bar{1}0]$  (the  $a$ -axis), with its top/bottom large surfaces being  $\pm(0001)$  and its side surfaces  $\pm(01\bar{1}0)$ . Due to the small thickness of 5 – 20 nm and large aspect ratio of  $\sim 1:4$ , the flexibility and toughness of the nanobelts are extremely high. A polar surface dominated nanobelt can be approximated as a capacitor with two parallel charged plates (Figure 2a). The polar nanobelt tends to roll over into an enclosed ring to reduce the electrostatic energy (Figure 2b). A spiral shape is also possible for reducing the electrostatic energy (Figure 2c) [11]. The formation of nanorings and nanohelices can be understood from the nature of the polar surfaces [10]. If the surface charges are uncompensated during growth, the spontaneous polarization induces electrostatic energy due to the dipole moment, whilst rolling up to form a circular ring would minimize or neutralize the overall dipole moment, reducing the electrostatic energy. On the other hand, bending of the nanobelt produces elastic energy. The stable shape of the nanobelt is determined by a minimization of the total energy contributed from spontaneous polarization and elasticity. If the nanobelt is rolled loop-by-loop, the repulsive force between the charged surfaces stretches the nanospring, while the elastic deformation force pulls the loops together; the balance between the two forms the nanospring that has elasticity (Figure 2d). The nanospring has a uniform shape with radius of  $\sim 500 - 800$  nm and evenly distributed pitches. Each is made of a uniformly deformed single-crystal ZnO nanobelt.

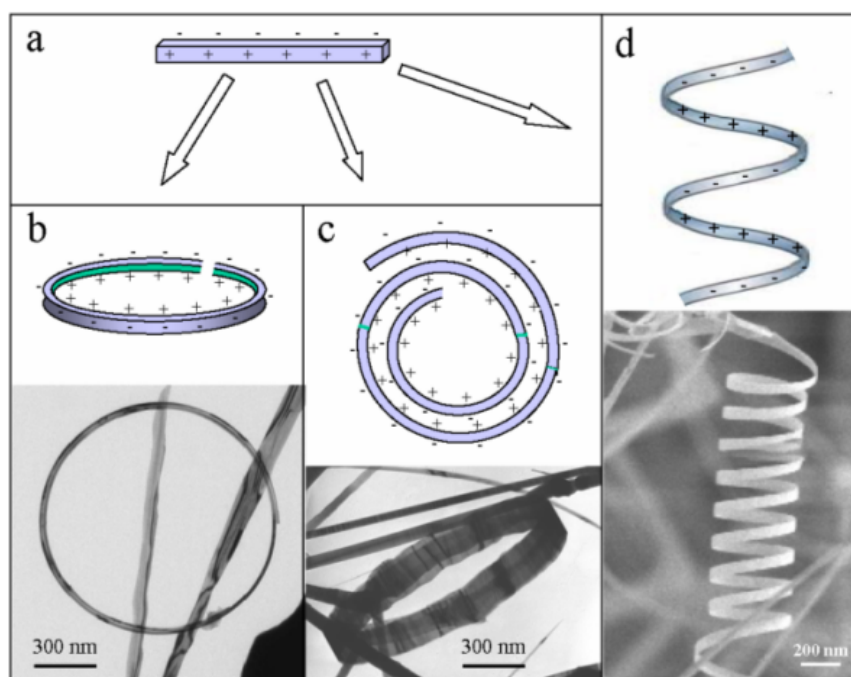


Figure 2. Stages of nanospring growth.

## 2.3 Nanobows

Nanobows are novel nanostructures found recently during the growth of nanorings. Continuous and uniform bending of nanobelts into semi-rings is a characteristic of all nanobows [12]. Figure 3(a) shows a

hexagonal ZnO rod with a ZnO nanobelt grown from one of its six primary crystallographic facets. The rod grows along  $[0001]$  with side surfaces of  $\{2\bar{1}\bar{1}0\}$  or  $\{01\bar{1}0\}$ . Based on growth of self-catalyzed ZnO nanostructures [13], the inner arc of the nanobelt is believed to be Zn-terminated while the outer surface is O-terminated. The image shows two nanobelts attached to one another prior to joining the hexagonal rod. These two nanobelts are  $120^\circ$  apart and are considered to exhibit opposite inner and outer surface terminations. Such assumptions are based on the single-crystal nature of nanobelts and the joining of the nanobelts at a common intersecting point. As illustrated by a schematic model (see the inset), the outside faces of the top and bottom nanobelts have Zn-terminated  $(0001)$  and O-terminated  $(000\bar{1})$  surfaces, respectively. At the junction between the two nanobelts, the negative inner surface of the top nanobelt corresponds to the negative outer surface of the bottom nanobelt. Electron diffraction recorded from the joint point of the nanobelt with the nanorod proves the single crystal structure of the entire entity (Fig. 3b).

We have proposed a mechanism about the formation of nanorings [10]. For a thin, straight polar-surface-dominated (PSD) nanobelt, the spontaneous polarization-induced electrostatic energy decreases upon rolling into a circular ring due to the neutralization of the dipole moment. The stable shape of the ring is dictated by the minimization of the total energy contributed by spontaneous polarization and elasticity.

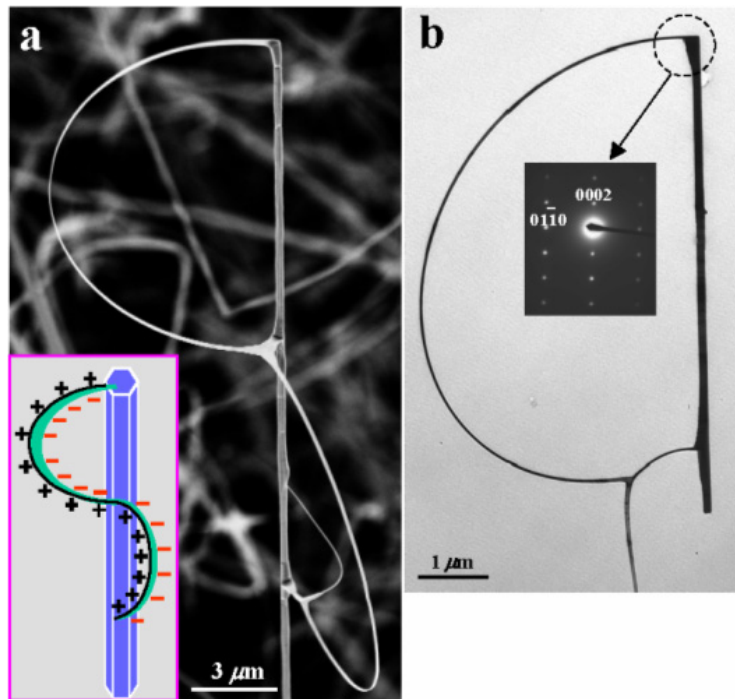


Figure 3. TEM images and schematic of nanobelts.

#### 2.4 Seamless nanorings

By adjusting the raw materials with the introduction of impurities, such as indium, we have synthesized a nanoring structure of ZnO (Fig. 4) [14]. TEM imaging indicates that the nanoring is a single-crystal entity with circular shape. The single-crystal structure referred here means a complete nanoring that is made of a single crystalline ribbon bent evenly at the curvature of the nanoring. Although the radius of the ring is large, its thickness is only  $\sim 10$  nm. The nanoring is made of a loop-by-loop co-axial, uni-radius, epitaxial-coiling of a nanobelt [14]. The growth of the nanoring structures can be understood from the polar surfaces of the ZnO nanobelt. The polar-nanobelt, which is the building block of the nanoring, grows in this instance along  $[10\bar{1}0]$ , with side surfaces  $\pm(1\bar{2}10)$  and top/bottom surfaces  $\pm(0001)$ , having a typical

width of  $\sim 15$  nm and thickness  $\sim 10$  nm. The nanobelt has polar charges on its top and bottom surfaces (Fig. 5a). If the surface charges are uncompensated during growth, the nanobelt may tend to fold itself as its length gets longer to minimize the area of the exposed polar surface. One possible way is to interface the positively charged Zn-(0001) plane (top surface) with the negatively charged O-(000 $\bar{1}$ ) plane (bottom surface), resulting in neutralization of the local polar charges and the reduced surface area, thus forming a loop with overlapping ends (Fig. 4b). This type of folding is  $90^\circ$  with respect to the folding direction for forming the nanospring or spiral nanostructure, possibly due to the difference in aspect ratio of the nanobelts and relative size of the polar surfaces. The radius of the loop may be determined by the initial folding of the nanobelt at the initial growth, but the size of the loop cannot be too small to reduce the elastic deformation energy. The total energy involved in the process comes from polar charges, surface area and elastic deformation. The long-range electrostatic interaction is likely to be the initial driving force for folding the nanobelt to form the first loop for the subsequent growth. This is the proposed mechanism for nucleation of the nanoring.

As the growth continues, the nanobelt may be naturally attracted onto the rim of the nanoring due to electrostatic interaction, extending parallel to the rim of the nanoring to neutralize the local polar charge and reduce the surface area, resulting in the formation of a self-coiled, co-axial, uni-radius, multi-looped nanoring structure (Fig. 5c). The self-assembly is spontaneous, which means that the self-coiling along the rim proceeds as the nanobelt grows. The reduced surface area and the formation of chemical bonds (short-range force) between the loops stabilize the coiled structure. The width of the nanoring increases as more loops wind along the nanoring axis, and all of them remain in the same crystal orientation (Fig. 5d). Since the growth was carried out in a temperature region of  $200\text{--}400^\circ\text{C}$ , “epitaxial sintering” of the adjacent loops forms a single-crystal cylindrical nanoring structure, and the loops of the nanobelt are joined by chemical bonds as a single entity. A uni-radius and perfectly aligned coiling is energetically favorable because of the complete neutralization of the local polar charges inside the nanoring and the reduced surface area. This is the “slinky” growth model of the nanorings [14]. The charge model of the nanoring is analogous to that of a single DNA helix.

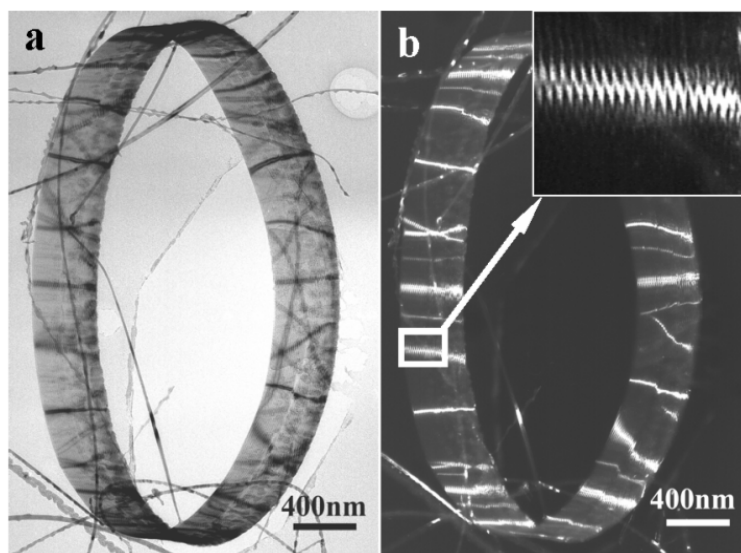


Figure 4. TEM images of nanorings.

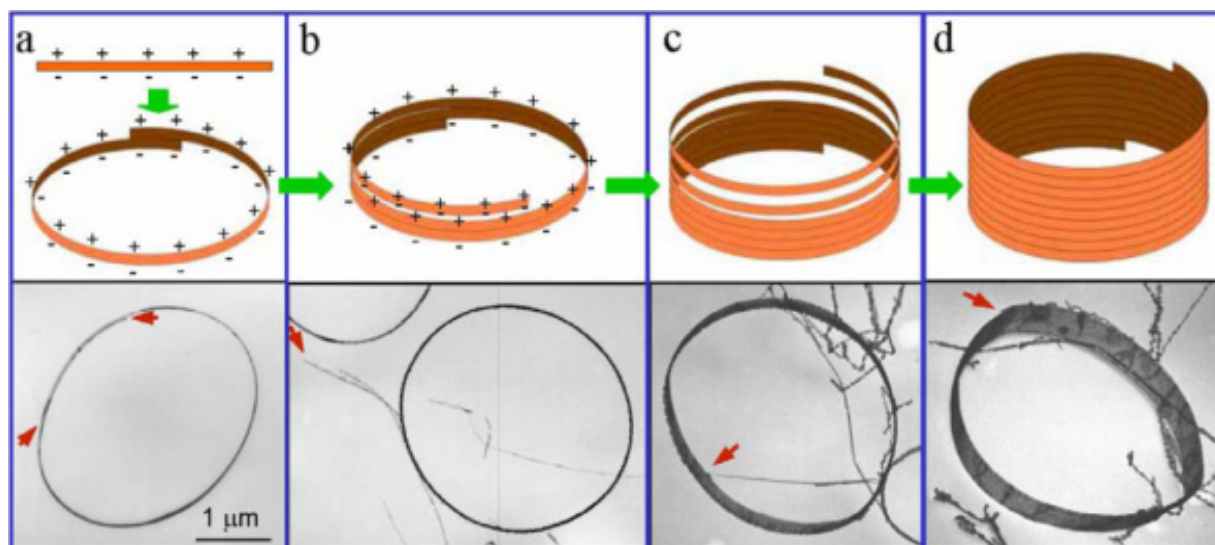


Figure 5. Mechanistic steps of seamless nanoring growth.

### 3. Summary

ZnO is unique because it exhibits semiconducting and piezoelectric dual properties. Structurally, ZnO is a material that has diverse structures, whose configurations are much more rich than any of the known nanomaterials including carbon nanotubes. Using a solid-state thermal sublimation process, and by controlling the growth kinetics, local growth temperature and the chemical composition of the source materials, a wide range of nanostructures of ZnO have been synthesized. These structures may have immeasurable potential in microsystem integration and biotechnology.

### 4. References

- [1] Pan Z W, Dai Z R and Wang Z L 2001 *Science* **209** 1947
- [2] Dai Z R, Pan Z W and Wang Z L 2003 *Adv. Functional Materials* **13** 9
- [3] Arnold M, Avouris P and Wang Z L 2002 *J. Phys. Chem. B* **107** 659
- [4] Comini E, Faglia G, Sberveglieri G, Pan Z W and Wang Z L 2002 *Applied Physics Letters* **81** 1869
- [5] Bai X D, Gao P X, Wang Z L and Wang E G 2003 *Appl. Phys. Letts.* **82** 4806
- [6] Hughes W and Wang Z L 2003 *Appl. Phys. Letts.* **82** 2886.
- [7] Shi L, Hao Q, Yu C, Kim D, Mingo N, Kong X Y and Wang Z L 2004 *Appl. Phys. Letts.* **84** 2638
- [8] Gao P X and Wang Z L 2002 *J. Phys. Chem. B* **106** 12653
- [9] Gao P X, Wang Z L 2004 *Appl. Phys. Letts* **84** 2883 + cover
- [10] Kong X Y and Wang Z L 2003 *Nano Letters* **3** 1625 + cover
- [11] Kong X Y and Wang Z L 2004 *Appl. Phys. Letts.* **84** 975 + cover
- [12] Hughes W and Wang Z L 2004 *J. Am. Chem. Soc.* submitted
- [13] Wang Z L, Kong X Y and Zuo J M 2003 *Phys. Rev. Letts.* **91** 185502 + cover
- [14] Kong X Y, Ding Y, Yang R S and Wang Z L 2004 *Science* **303** 1348